Diversity and phylogeny of gephyrin: Tissue-specific splice variants, gene structure, and sequence similarities to molybdenum cofactor-synthesizing and cytoskeleton-associated proteins

Markus Ramming*†, Stefan Kins*‡, Nikos Werner, Achim Hermann, Heinrich Betz, and Joachim Kirsch§

Department of Neurochemistry, Max-Planck-Institute for Brain Research, Deutschordenstr. 46, 60528 Frankfurt am Main, Germany

Edited by Solomon H. Snyder, Johns Hopkins University School of Medicine, Baltimore, MD, and approved June 19, 2000 (received for review September 10, 1998)

Gephyrin is essential for both the postsynaptic localization of inhibitory neurotransmitter receptors in the central nervous system and the biosynthesis of the molybdenum cofactor (Moco) in different peripheral organs. Several alternatively spliced gephyrin transcripts have been identified in rat brain that differ in their 5′ coding regions. Here, we describe gephyrin splice variants that are differentially expressed in non-neuronal tissues and different regions of the adult mouse brain. Analysis of the murine gephyrin gene indicates a highly mosaic organization, with eight of its 29 exons corresponding to the alternatively spliced regions identified by cDNA sequencing. The N- and C-terminal domains of gephyrin encoded by exons 3–7 and 16–29, respectively, display sequence similarities to bacterial, invertebrate, and plant proteins involved in Moco biosynthesis, whereas the central exons 8, 13, and 14 encode motifs that may mediate oligomerization and tubulin binding. Our data are consistent with gephyrin having evolved from a Moco biosynthetic protein by insertion of protein interaction sequences.

glycine receptor | γ-aminobutyric acid type A receptor | receptor clustering | tubulin binding | evolution

Gephyrin originally was identified as a membrane-associated protein of 93 kDa that copurifies with the mammalian inhibitory glycine receptor (GlyR) (1–3). In spinal cord and brain, gephyrin decorates the cytoplasmic face of postsynaptic membrane specializations containing a high density of GlyRs or closely related γ-aminobutyric acid type A ($GABA_A$) receptors (4–6). Biochemical and cotransfection studies have revealed that gephyrin can interact with polymerized tubulin (7) as well as the β subunit of the GlyR (8, 9) and, to a lesser extent, the β3 subunit of $GABA_A$ receptors (10). Gephyrin therefore is thought to anchor inhibitory neurotransmitter receptors to the cytoskeletal structures underlying postsynaptic membrane differentiations (2, 3, 7, 11). Consistent with this view, the postsynaptic localization of gephyrin is altered by alkaloids affecting the integrity of the cytoskeleton (11).

Different lines of evidence indicate that gephyrin is essential for the synaptic localization of both GlyRs and $GABA_A$ receptors. In cultured primary neurons, the accumulation of gephyrin at developing postsynaptic sites precedes receptor clustering (12–14), and inhibition of gephyrin expression by antisense oligonucleotides prevents the synaptic localization of both GlyRs (12) and $GABA_A$ receptors (15). Furthermore, neurons from gephyrin knockout mice display a total loss of postsynaptic staining for GlyR α (16) and $GABA_A$ receptor α2 and γ2 (17) subunits. Conversely, $GABA_A$ receptor γ2 subunit-deficient mice show a strong reduction in postsynaptic gephyrin and $GABA_A$ receptor clusters (15). These data are consistent with an organizer role of gephyrin at inhibitory synapses (14, 18).

Recent reports demonstrate that gephyrin also has a nonsynaptic function in intermediary metabolism. Both the N- and C-terminal regions of gephyrin display highly significant sequence similarities to bacterial (3, 19), invertebrate (20), and plant (21) proteins involved in the biosynthesis of the molybdenum cofactor (Moco), which forms the prosthetic group of nearly all molybdoenzymes (22). In liver and intestine of mouse embryos deficient for gephyrin, the activities of the Moco-dependent enzymes xanthine dehydrogenase and sulfite oxidase are reduced to background levels (16). Also, expression of the N-terminal region of gephyrin has been found to rescue the phenotypes of Moco biosynthesis mutants in both *Escherichia coli* and plants (23). These data indicate that gephyrin is required for Moco biosynthesis, a finding that explains the constitutive transcription of the gephyrin gene in all mammalian tissues examined so far (3, 24). Interestingly, patients suffering from hereditary Moco deficiency display symptoms that resemble those seen upon loss of inhibitory neurotransmission, including myoclonus and epileptic seizures. In addition, the patients suffer from severe neurological abnormalities, microcephaly, and mental retardation (25). Thus, the Moco biosynthetic function of gephyrin may be important for brain development.

The molecular basis for gephyrin's distinct functions is only poorly understood. Previous work from our laboratory has identified alternatively spliced gephyrin transcripts in rat brain and spinal cord, which differ by four short nucleotide sequences (C1–C4) in the 5′ coding region (3). Here, we describe additional gephyrin splice variants that are differentially expressed in brain and peripheral organs. The analysis of murine genomic DNA presented in this paper indicates that these mRNAs are generated from a highly mosaic gene that contains several phylogenetically old exons. Therefore, gephyrin may have acquired multifunctionality by recruiting novel exonic sequences into the

---

This paper was submitted directly (Track II) to the PNAS office.

Abbreviations: $GABA_A$, γ-aminobutyric acid type A; GlyR, glycine receptor; Moco, molybdenum cofactor.

Data deposition: The sequences reported in this paper have been deposited in the GenBank database (accession nos. AJ278768, AJ278769, and AJ278770).

*M.R. and S.K. contributed equally to this work.

†Present address: Hoechst-Marion-Roussel, 65903 Frankfurt, Germany.

‡Present address: Department of Psychiatric Research, University of Zürich, August-Forel-Str. 1, CH-8008 Zürich, Switzerland.

§To whom reprint requests should be sent at present address: Department of Anatomy and Cellular Neurobiology, University of Ulm, Albert-Einstein-Allee 11, D-89069 Ulm, Germany. E-mail: joachim.kirsch@medizin.uni-ulm.de.

The publication costs of this article were defrayed in part by page charge payment. This article must therefore be hereby marked "*advertisement*" in accordance with 18 U.S.C. §1734 solely to indicate this fact.

region that joins the ancestral sequences of invertebrate Moco synthesizing proteins.

Materials and Methods

Library Screening. Murine gephyrin cDNAs were isolated from a mouse brain cDNA library (1.5×10^6 plaque-forming units) constructed in the phage λ-ZAPII (Stratagene) by screening with a randomly primed ^{32}P-labeled rat gephyrin cDNA (clone p2) lacking the poly(A)$^+$ tail under moderately stringent conditions as described (3).

Northern Blot Analysis. Murine multiple tissue Northern blot membranes (CLONTECH) were probed with synthetic oligonucleotides corresponding to either the 3′ end of the gephyrin coding region (T1) or cassettes C1–C4 (26). Gephyrin transcripts containing cassettes C5–C7 were detected with the following antisense probes: 5′-TGGACTGGACTCTTAAGTCGTAGCCTCTATTCCTCCAGAGTTCAT-3′ (C5), 5′-ATTCCTCTGTGGTCTCTGCTTCAGTTCCTGCCTTGAGTGCCTGCC-3′ (C6), and 5′-ATCTGAGGCTACTTTCTTGTTGGTATGTGTACCTCAGCCTGCTGC-3′ (C7). Oligonucleotides were 5′-labeled by using polynucleotide kinase (Boehringer Mannheim) and γ[^{32}P]dATP (Amersham Pharmacia). Hybridization conditions were as for library screening; high stringency washes were performed at 65°C. Autoradiographs were exposed for 24–72 h on Biomax film (Kodak).

***In Situ* Hybridization.** Oligonucleotide probes were 3′ end-labeled to identical specific activities (5×10^8 to 1×10^9 dpm/μg) by using terminal transferase (Amersham Pharmacia) and α[^{35}S]dATP (Amersham Pharmacia). The same oligonucleotides as for Northern blot analysis were used. Control hybridizations were performed as described (26). Tissue sections were exposed for 6–8 weeks on X-Omat film at room temperature.

Screening of Genomic Libraries and Clone Analysis. Exonic sequences were isolated by screening a BALB/c mouse genomic library (27) constructed in the phage vector λ-Fix (kindly donated by B. Sommer, University of Heidelberg, Germany) and a 129/SV mouse genomic library constructed in the λ-FixII vector (Stratagene) by using ^{32}P-labeled PCR fragments corresponding to nucleotides 1–330, 475–717, 1309–1665, 2137–2215, and 2479–2839 of clone p2 (3) as hybridization probes. Positive phages were verified by Southern blotting of enzymatic digests, followed by hybridization with a panel of ^{32}P-labeled oligonucleotide probes, derived from different regions of the rat gephyrin cDNA (3). Hybridizing bands were subcloned into pBluescript SK+ (Stratagene). Additional fragments were identified by PCR screening of a P1-library (Genome Systems, St. Louis) by using oligonucleotide primers derived from genomic sequences adjacent to the missing exons.

DNA Sequencing. Nucleotide sequences were determined by the dideoxy chain termination method using either a T7-sequencing kit (Amersham Pharmacia) or a DyeDeoxy Terminator Cycle sequencing kit (Applied Biosystems). All exonic sequences were confirmed by analyzing both DNA strands.

Results

Identification of Gephyrin Splice Variants. To disclose the full complexity of gephyrin transcripts, we first searched for novel gephyrin cDNAs. Low stringency screening of a mouse brain cDNA library resulted in the identification of 48 hybridization-positive clones. Restriction analysis revealed three clones (p8–p10) with novel alternatively spliced regions, named C5–C7, which encompass 60 bp, 120 bp, and 67 bp, respectively (Fig. 1*A*). Insertion of these sequences alters the predicted primary structure of gephyrin. In transcripts containing region C5, the ORF

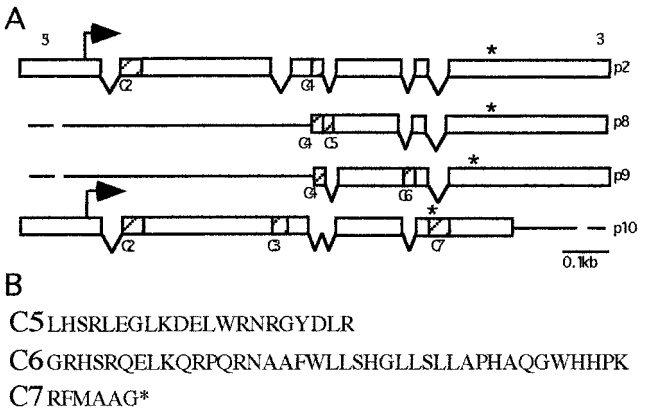

Fig. 1. Identification of alternative spliced regions C5–C7. (*A*) Schematic representation of the gephyrin cDNA and clones p8–p10 containing novel nucleotide sequences. Exonic regions are displayed as boxes, intronic sequences are shown as a line. Dotted lines indicate only partially sequenced introns. Alternatively spliced regions are represented by hatched boxes, and initiation and stop codons are marked by arrows and asterisks, respectively. The alternatively spliced region C4b has been identified by Heck *et al.* (28). (*B*) Deduced amino acid sequences of regions C5–C7. The first aa shown is encoded by the preceding exon.

is conserved, resulting in a protein that is 20 aa longer (Fig. 1*B*). In addition, between the alternatively spliced regions C4 and C5 an alternatively spliced sequence (C4b) has been identified, which creates a consensus site for protein kinase C phosphorylation (28). Insertion of sequence C6 (Fig. 1*B*) generates a 40-aa motif that contains many positively charged amino acids and displays no significant sequence similarity to known polypeptides. Use of region C7 (Fig. 1*B*) leads to a stop codon after only five additional amino acids, thus generating a truncated gephyrin isoform.

Structure of the Murine Gephyrin Gene and Protein. To unravel the molecular basis for gephyrin transcript diversity, we analyzed the structure of the mouse gephyrin gene. Screening of BALB/c and 129/SV mouse genomic libraries resulted in the isolation of 11 independent λ-phages, which covered 18 exons of the mouse gephyrin gene. Further analysis of four P1 clones disclosed the full exonic organization (Fig. 2*A*). Accordingly, and consistent with transcription start site mapping data (24), its transcribed region is dispersed over 29 exons, most of which encode only 20–40 aa. The sizes of the separating introns range between 0.4 and 13 kb, with the total length of the gene being >150 kb (Table 1). All exons have splice acceptor and donor sites that match the mammalian consensus sequences (29). The alternatively spliced regions C1–C7 (including C4b) correspond to exons 2, 3, 9, 11, 12, 13, 19, and 21.

Inspection of the mouse and rat sequences revealed an astoundingly high extent of interspecies conservation. The coding regions of the mouse gephyrin gene are 97.2% identical with the rat cDNA. Alignments of the deduced primary structures of rat and mouse gephyrin identified only two amino acid substitutions. In region C3, asparagine 265 and valine 274 are replaced by lysine and leucine, respectively. In contrast, nucleotides 1–120 in the 5′ untranslated region of the rat cDNA clone p1 (3) lack significant sequence similarity to the corresponding region of mouse exon 1. Two consensus polyadenylation signals are identified 830 and 960 bp downstream from the splice acceptor site of exon 29. The first of these positions coincides with the polyadenylation signal found in the rat gephyrin cDNA (3).

Sequence Similarities of Gephyrin to Other Proteins. The C-terminal half of rat and mouse gephyrin displays striking sequence

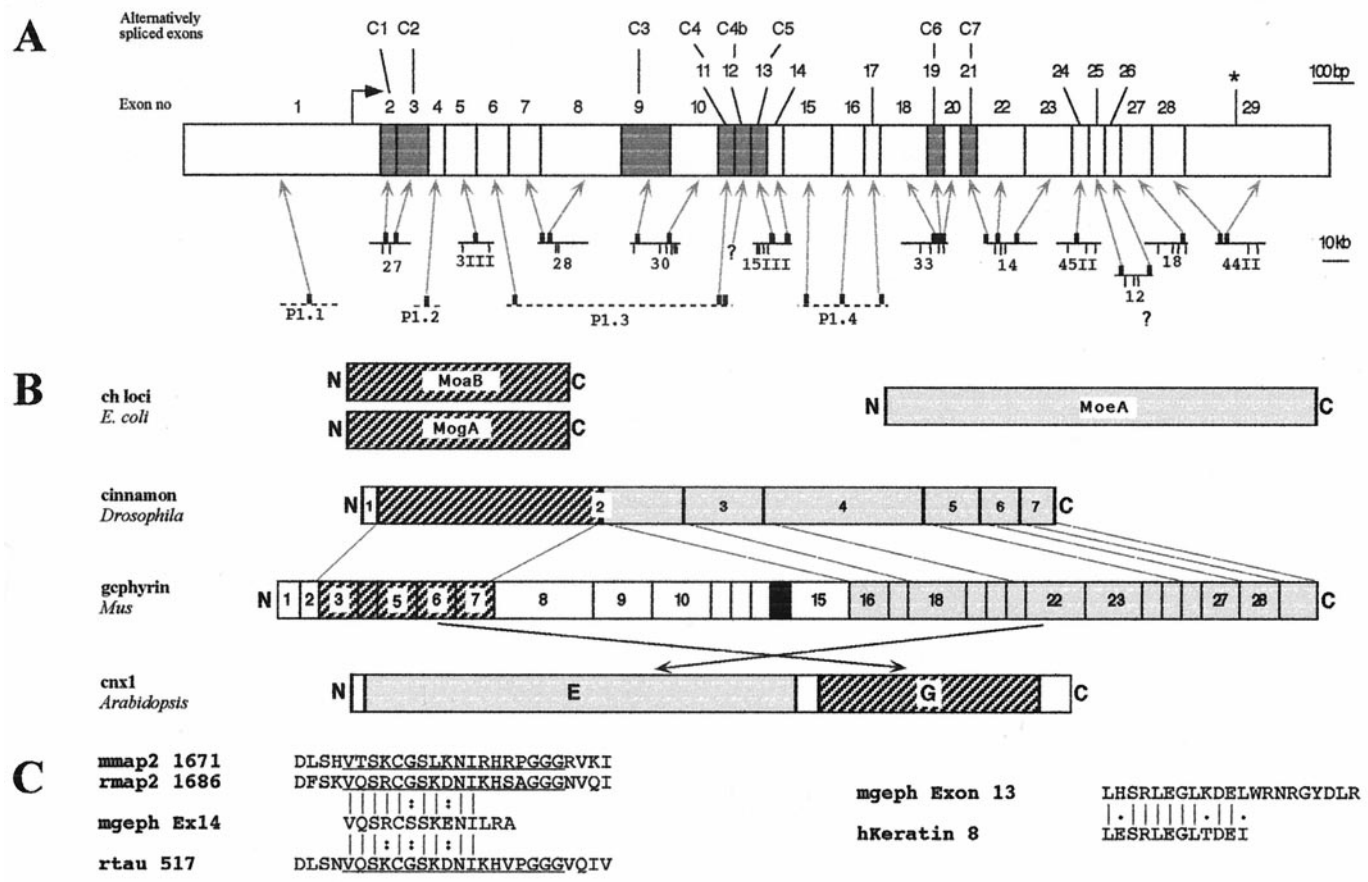

Fig. 2. Structure of the murine gephyrin gene and domain analysis of the encoded protein. (*A*) Exon positions and relevant restriction sites of murine gephyrin genomic DNAs. (*Upper*) The exon borders of the gephyrin gene are projected onto a schematic representation of the gephyrin cDNA. An arrow marks the initiation codon, an asterisk the stop signal. Gray boxes indicate the alternatively spliced exons C1–C7. (*Lower*) Positions and lengths of genomic clones. Arrows indicate the relative positions of the exonic sequences on the isolated λ phages (solid lines) and P1 clones (dashed lines). Clone numbers and *Eco*RI restriction sites (vertical bars) used for mapping are indicated. Note different scales of size bars for both representations. (*B*) Comparison of the exon-intron boundaries and domains of gephyrin with sequence similarities to bacterial, invertebrate, and plant Moco proteins. Boxes and numbers within cinnamon and gephyrin correspond to the exons of the respective genes. Dashed and gray boxes indicate regions with sequence similarities to the bacterial proteins MoaB/MogA and MoeA, respectively. The black box in the central region of gephyrin indicates the region displaying sequence similarity to microtubule associated proteins encoded by exon 14. Dashed lines mark exon/intron boundaries conserved between cinnamon and gephyrin. Crossed arrows indicate swapping of the MoaB/MogA and MoeA homology domains in cnx 1 as compared with cinnamon and gephyrin. (*C*) Alignment of the amino acid motifs encoded by exons 13 and 14 of the murine gephyrin gene with the core repeat motif of MAP2 and tau and the oligomerization domain of keratin 1B. The motif encoded by exon 14 aligns well with the second imperfect octadecapeptide repeat of the microtubule-associated proteins MAP2 from mouse (mmap2), MAP2 from rat (rmap2) and tau from rat (rtau) and the C-terminal sequence predicted from exon 13 aligns well with the oligomerization domain of keratin 1B. Identical residues are indicated by dashes, and isofunctional ones by two dots.

similarity (36% amino acid identity) to the MoeA (chlE) protein *of E. coli* (3). The corresponding gene maps to the chlorate-resistent loci (chl) of *E. coli* and the encoded protein is involved in the biosynthesis of molybdopterin, a biosynthetic precursor of Moco. Significant sequence similarity also exists between the N-terminal half of gephyrin and two other proteins of the chl loci of *E. coli*, MoaB (chlA2) and MogA (chlG) (30). The regions of gephyrin corresponding to these *E. coli* gene products are encoded by exons 3–7 and 16–29, respectively (Fig. 2*B*) and show high sequence similarity to the Moco biosynthetic proteins cinnamon of *Drosophila melanogaster* (20) and cnx1 of *Arabidopsis thaliana* (21). Comparison of the structures of the gephyrin and cinnamon genes indicates that all but the last of the five intron/exon boundaries of the cinnamon gene (20) are precisely conserved in the murine gephyrin gene (Fig. 2*B*). Only the boundary of the last exon of cinnamon is shifted by 6 nt. Notably, only three of the eight alternatively spliced exons (exons 3, 19, and 21) of the gephyrin gene lie within the Moco protein homology domains. Two of these (exon 3 corresponding to C2 and exon 19 corresponding to C6) encode abundantly expressed sequences, with insertion of exon 21 (C7), resulting in a truncated gephyrin isoform. All other alternatively spliced regions with the exception of C1 lie within the central domain of gephyrin that is unique to this mammalian gene product.

Interestingly, several of the exons found in the central portion of the murine gephyrin gene encode sequences that may mediate protein–protein interactions. Exon 8 encodes the core of the previously identified region (3) rich in hydroxylated, charged, and proline residues (amino acids 174–243) that has been proposed to bind profilin (34). From the alternatively spliced exon 13 corresponding to region C5, a protein sequence is predicted that shows striking sequence similarity (Fig. 2*C*) to a small part of the α-helical dimerization domain 1B of human keratin 8 (31). Exon 14 translates into an amino acid motif (Fig. 2*C*) that is 80%, and 60%, identical to the second imperfect repeat motifs of the rat microtubule-associated proteins MAP2 (32) and tau (33). These repeat motifs of tau and MAP2 have been shown to promote tubulin polymerization and to mediate

Table 1. Exon-intron boundaries of the mouse gephyrin gene

Exon no.	Exon length, bp	Acceptor site	Donor site	Size of 3′ intron, kb
1	64		ACAG*gt*aacgg	>7
2 (C1)	58	tgg*ag*GCCA	TTGG*gt*gtcg	~5
3 (C2)	79	ttt*ag*TGAG	CTTT*gt*gagt	>6
4	58	tcc*ag*Gtt	CAAG*gt*ata	>7
5	93	ttt*ag*GAA	AGAG*gt*gag	>6
6	95	tat*ag*GCC	CTAG*gt*aag	>2
7	67	ttc*ag*ACC	TCAG*gt*aag	~1.5
8	273	ggc*ag*GAA	AAAG*gt*aagt	>10
9 (C3)	108	att*ag*AAGC	ACGG*gt*aag	~13
10	135	ttt*ag*ATTC	AAAA*gt*aagt	>5
11 (C4)	42	acc*ag*GCTCG	TGAG*gt*ata	>5
12 (C4b)*	57	—	—	n.d.
13 (C5)	60	actagCTCCA	AAGAgtaac	n.d.
14	43	tgc*ag*GTCCA	GCCA*gt*aatg	>5
15	138	ttt*ag*GTCA	CGAG*gt*actt	>4
16	93	ttc*ag*ATGGA	CGAG*gt*aaat	>3
17	56	cac*ag*CTGCTG	GCAG*gt*gag	>10
18	120	ttc*ag*CCAACT	TGAT*gt*atgt	~1
19 (C6)	119	gtt*ag*GGCAGG	CAAA*gt*aag	~1
20	59	tat*ag*GGTACT	TCCG*gt*aagt	0.4
21 (C7)	67	cac*ag*CTTTAT	TAAGgtgtct	~3.5
22	154	ttc*ag*ACCCAT	TGAG*gt*aaat	>3
23	122	tgt*ag*CTGCTA	ACAA*gt*atg	>6
24	88	tcc*ag*CCCAGA	AAAG*gt*atga	>6
25	74	tgc*ag*GACTA	CAGG*gt*atga	~10
26	65	tct*ag*CTTGCG	CCAG*gt*aagg	~13
27	104	ttc*ag*GGAATC	CAGG*gt*aatgt	>3
28	97	tgt*ag*TTATCG	ACAG*gt*cagtc	~2
29	131	tcc*ag*GTAATC		

Intron sequences are indicated in lowercase letters, with the donor and acceptor sequences in italics. The capital letters correspond to the exonic sequences. The sizes of each exon and it 3′ adjacent intron are indicated; the numbers of bp given for the first and the last exon correspond only to the respective coding sequences. n.d., not determined.
*Region identified by Heck *et al.* (28).

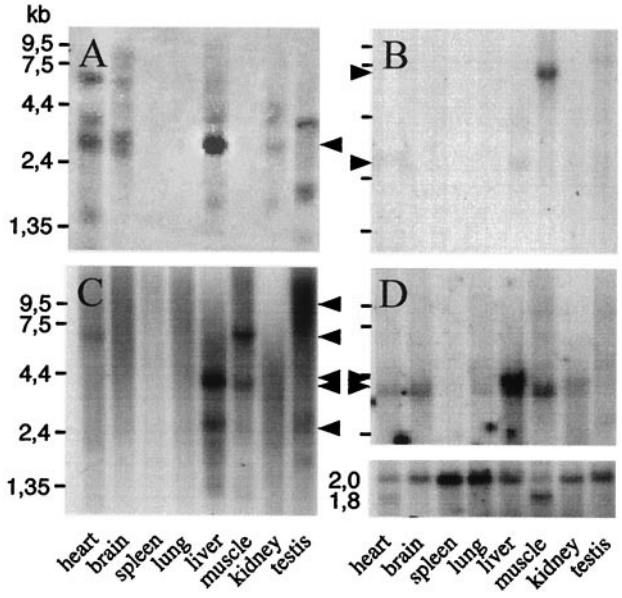

Fig. 3. Distribution of alternatively spliced gephyrin sequences in murine non-neuronal tissues and brain. Oligonucleotide probes specific for the alternatively spliced exons 3 (C2: *A*), 13 (C5: *B*), 19 (C6: *C*), and the invariant 3′ region of the murine gephyrin mRNA (T1: *D Upper*) as well as for β actin transcripts (*D Lower*) were hybridized to a multiple tissue Northern blot. The exon 3 probe revealed a predominant 3.8-kb transcript in liver in addition to differentially spliced mRNAs in heart, brain, liver, kidney, and testis (*A*). The exon 13 probe hybridized to a mRNA of 6.5 kb in muscle and heart (*B*). Expression of transcripts containing exon 19 (*C*) was seen in liver (3.8 and 2.2 kb), skeletal muscle (6.5 and 3.6 kb), and possibly testis (≈9 kb and 2.2 kb). In addition, higher molecular weight mRNAs were detected in heart (6.5 kb). In brain, heterogeneous bands 5–9 kb were labeled. The T1 probe detected 3.6- to 3.8-kb RNAs in all tissues examined except spleen (*D Upper*). Control hybridizations obtained with a probe specific for β actin transcripts also are shown (*D Lower*).

microtubule binding. The domain of gephyrin encoded by exon 14 is therefore likely to mediate its high-affinity interaction with polymerized microtubules (7).

Northern Analysis. To confirm expression of the alternatively spliced exons of the gephyrin gene, we performed Northern hybridizations with exon-specific synthetic oligonucleotides. Previously, using a randomly labeled gephyrin cDNA we had identified a major gephyrin mRNA of 3.5–3.7 kb in brain, liver, lung, and kidney (3). Consistent with these data, hybridization of a Northern blot of poly(A)$^+$ RNA isolated from brain, heart, skeletal muscle, spleen, liver, lung, kidney, and testis with the T1 oligonucleotide (exon 28) revealed 3.6–3.8 kb mRNAs in all organs except spleen (Fig. 3*D Upper*). However, liver displayed a much stronger signal than all other organs examined. Additional transcript heterogeneity was revealed by sequentially hybridizing cassette-specific synthetic oligonucleotides to a multiple tissue Northern blot (Table 2). A dominant hybridization signal at 3.6–3.8 kb in liver, brain, muscle, heart, kidney, lung, and testis was obtained with an exon 3 probe (C2; Fig. 3*A*). An exon 19 (C6; Fig. 3*C*) specific oligonucleotide hybridized to 3.6- to 3.8-kb transcripts in muscle and liver. These mRNAs were also weakly labeled by the exon 9 (C3) probe (Table 2). Low levels of a 5.1-kb transcript were detected by an exon 2 (C1) probe in all organs, whereas an oligonucleotide complementary to exon 11 (C4) gave a weak hybridization with an identically sized mRNA in liver only (Table 2). An even larger transcript of about 6.5 kb was visualized by the C2 (exon 3) probe in heart and, upon prolonged exposure, skeletal muscle; an identically sized transcript also hybridized with the exon 9 (C3) probe in muscle and with exon 13 (C5) and exon 19 (C6) sequences in both muscle and heart. Additional mRNA species of 4.2 kb containing exon 3 (C2) were found in heart, liver, kidney, and testis (Fig. 3*A*). Heterogeneous about 9 kb (exon 19; Fig. 3*C*) transcripts in testis and some shorter (*ca.* 2.2–2.6 kb) RNAs species that hybridized to the exon 3 (C2) and exon 19 (C6) probes also were detected. The former may correspond to incompletely processed pre-mRNAs, whereas the latter may represent degradation products of the major 3.6- to 3.8-kb transcript (see ref. 3). Together, these results indicate a widespread and differential expression of alternatively spliced gephyrin mRNAs in various tissues and highlight the potential complexity of gephyrin isoforms.

***In Situ* Hybridization.** Previous work has revealed abundant expression of gephyrin transcripts containing the exon 3 (C2) sequence in all synaptic regions of the rat brain, whereas exon 9 (C3)-specific and exon 11 (C4)-specific probes produced only weak labeling of cells in hippocampus and cerebellum (26). To visualize the distribution of the other alternatively spliced gephyrin mRNAs in mouse brain, we hybridized the radiolabeled oligonucleotide T1 (exon 28) and probes specific for regions C1 and C5–C7 to sagittal and horizontal brain sections (Fig. 4). As described previously for rat (26), T1 signals were ubiquitously present in the gray matter of the brain. Strongest hybridization was seen in olfactory bulb, the granular layer of the cerebellum, and hippocampus, whereas cortex, caudate putamen, and dien-

NEUROBIOLOGY

Table 2. Tissue distribution of alternatively spliced gephyrin sequences

Probe	Brain	Muscle	Heart	Liver	Lung	Spleen	Kidney	Testis
Exon 2 (C1)	(5.1)	(5.1)	(5.1)	(5.1)	(5.1)	(5.1)	(5.1)	(5.1)
Exon 3 (C2)		(6.5)	6.5		n.d.	n.d.		
	3.6	3.6	3.6	3.8			3.6	3.6
Exon 9 (C3)	n.d.	(6.5)	(6.5)		n.d.	n.d.		4.5
		3.6	3.6	3.8	(3.8)		3.6	3.6
Exon 11 (C4)	n.d.	n.d.	n.d.	5.1	n.d.	n.d.	n.d.	n.d.
Exon 13 (C5)	n.d.	6.5	(6.5)	n.d.	n.d.	n.d.	n.d.	n.d.
Exon 19 (C6)	5–9	6.5	6.5		n.d.	n.d.		≈9
		3.6	3.6	3.8			3.6	3.6
Exon 21 (C7)		6.5						
	5.1	5.1	5.1	5.1	5.1	5.1	5.1	5.1

The numbers indicate the lengths of the gephyrin transcripts in kb as detected with the probes indicated. A exon 11-specific probe cross-hybridized strongly to a band of 1.6 kb in all tissues examined; the nature of this transcript is presently unclear. Parentheses indicate RNAs of low abundance. Putative degradation products (2.2–2.6 kb) of the major 3.6- to 3.8-kb gephyrin transcript are not included. n.d., no transcripts detected.

cephalon showed moderate labeling. Consistent with our earlier findings (26), the exon 2 (C1) probe produced only very weak signals in the olfactory bulb and the granular layer of the cerebellum, both regions of high neuron density (Fig. 4). A similar hybridization pattern also was obtained with the exon 13 (C5)-specific oligonucleotide, although Northern analysis had revealed C5 transcripts in muscle only. Thus, these signals may correspond to low abundance RNAs that are highly expressed in some subpopulations of neurons. Transcripts hybridizing to the exon 19 (C6)-specific oligonucleotide were found throughout the gray matter, with distribution patterns resembling that obtained with probe T1 (not shown) or the earlier used C2 and T2 oligonucleotides (26). Because the C6 oligonucleotide did not hybridize to a discrete band in Northern blots of brain RNA, these signals may not be specific. The C7 (exon 21) probe produced only weak signals in the granular layer of the cerebellum and the olfactory bulb, with more prominent labeling of the medial habenula (Fig. 4). In conclusion, of the known alternatively spliced exons, only exon 3 sequences appear to be abundantly represented in brain gephyrin transcripts.

Discussion

In this study, we describe three alternatively spliced exons of the murine gephyrin gene and show that the corresponding transcripts are differentially expressed in brain and non-neuronal tissues. Our data extend the previously noted diversity of gephyrin transcripts and demonstrate that the latter results from a highly mosaic gene organization.

Inclusion of exons 3, 19, and 21 into the gephyrin mRNA has significant implications for the primary structure of the resulting polypeptides. Exon 13 encodes an amino acid motif with strong sequence similarity to the α-helical region 1B of human keratin 8 (31). The latter is known to mediate keratin dimerization by the formation of coiled-coil structures. Therefore, exon 13 may provide a domain of gephyrin involved in homo-oligomerization or interaction with other polypeptides. Exon 19 translates into a sequence of 40 aa characterized by many positively charged and a cluster of hydrophobic amino acids. In contrast, the presence of exon 21 leads to a C-terminally truncated form of gephyrin, which remains to be identified at the protein level.

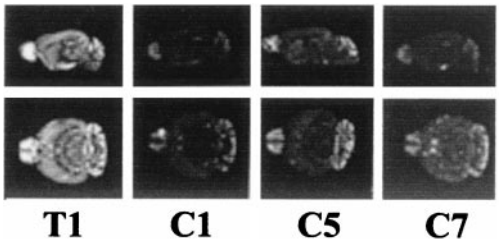

Fig. 4. *In situ* hybridization analysis. Autoradiographs of parasagittal (*Upper*) and horizontal (*Lower*) sections of adult mouse brain were hybridized to ^{35}S-labeled oligonucleotides specific for exons 2 (C1), 13 (C5), 21 (C7), and the T1 region (exon 28) of the gephyrin mRNA. Note similar labeling patterns of the C1, C5, and C7 probes.

Previous Northern blot analyses with a labeled cDNA probe had revealed major gephyrin transcripts of 3.5–3.7 kb in different organs (3). Here, exon-specific oligonucleotides disclosed additional variability in gephyrin transcript lengths, covering a range of mRNAs from 2.2 kb to 6.5 kb in size. At present, the physiological roles of these mRNAs are unknown. However, it is noteworthy that a particularly high diversity of gephyrin transcripts was observed in skeletal muscle, heart, liver, and brain. Transcripts of 3.6–3.8 kb (and 5.1 kb) were found in all organs (with the possible exception of spleen), whereas larger 6.5-kb mRNAs were seen only in excitable tissues, i.e., brain, heart, and skeletal muscle. This finding is consistent with abundant expression of Moco-dependent enzymes in liver and muscle and supports the notion that gephyrin may subserve both synaptic and metabolic functions in the nervous system.

Analysis of genomic DNA revealed a highly mosaic organization of the murine gephyrin gene and confirmed that all alternatively spliced regions of the gephyrin mRNA are encoded by separate exons. From the clones analyzed presently, we estimate that the murine gene is spread over >150 kb of genomic DNA. Its coding region is dispersed over 29 exons, which are separated by introns of 0.4 to >13 kb in size. At least eight of these exons are subject to alternative splicing, as indicated by sequencing of gephyrin cDNAs isolated from rat and mouse brain. Notably, the murine gephyrin gene displays a much higher extent of mosaicism than the related cinnamon gene of *Drosophila*. This may reflect both the acquisition of novel functions by insertion of additional exons in the central region of the gene and the polymorphism of its secondary transcripts.

It has been previously (3, 20, 21) noted that the N- and C-terminal regions of gephyrin are similar to gene products catalyzing distinct steps in the biosynthesis of Moco and its precursor molybdopterin (22). These include the three *E. coli* polypeptides MoeA, MogA, and MoaB (19, 30), the *Drosophila* protein cinnamon (20), and the cnx-1 protein of *A. thaliana* (21). Whereas in *E. coli* the individual reactions of the Moco pathway are controlled by individual gene products, cinnamon is thought to be capable of catalyzing multiple steps (20). This is consistent with its two-domain structure, in which a region with sequence

similarity to the MoaB and MogA proteins appears to be fused to a domain similar to MoeA. The order of these domains (termed G- and E-domains) is swapped in the plant protein cnx-1 (see Fig. 2*B*). Consistent with a conserved function of these sequence similarity domains, the N-terminal MogA homology domain is capable of rescuing Moco biosynthesis mutants of *E. coli* and *Arabidopsis*. Furthermore, all but one of the exon/intron boundaries of the *Drosophila* cinnamon gene are precisely conserved in the murine gephyrin gene, thus corroborating the close evolutionary relation of these genes despite their differences in size and extent of mosaicism. These findings underline the old phylogenetic origin of large regions of the gephyrin gene and the considerable evolutionary pressure involved in its conservation. Furthermore, they are consistent with an evolutionary scheme, in which an archaic protein encoded by an ancestral gephyrin gene acquired synaptic functions by recruiting novel exons into the region that connects the bacterial precursor sequences of Moco synthesizing proteins from invertebrates.

The functions of these phylogenetically young exons of the gephyrin gene are largely unknown. However, as outlined above, the protein domains encoded by exons 8 and 13 are likely to mediate interactions with other proteins. Gephyrin has been shown to interact with a number of synaptic membrane and signaling proteins, including the glycine receptor β subunit (8, 9), the actin binding protein profilin (34), the translational regulator RAFT1 (35), and the recently discovered GDP/GTP exchange factor collybistin (36). For none of these proteins, its binding site on gephyrin has been elucidated. Also, detergent-solubilized gephyrin shows a high tendency to form aggregates (2), a property that may be crucial for the formation of postsynaptic gephyrin clusters (4, 6, 11–15). These observations are consistent with the demonstration of a trimeric arrangement of MogA (38). Finally, gephyrin binds with high affinity to polymerized tubulin (7). This interaction is likely to involve the amino acid sequence motif encoded by exon 14, which displays high sequence similarity to the core repeats of the microtubule binding domains of MAP2 and tau. MAP2 and tau both contain three nonidentical octadecapeptide repeats, which all contribute to microtubule binding (32, 33). Notably, the seven C-terminal amino acids of these octadecapeptide repeats, which are not conserved in gephyrin, are unlikely to interact with the microtubular surface, because a mAb raised against this conserved epitope fails to block microtubule binding, but cosediments with microtubules (37). Because gephyrin has only a single "repeat" motif, gephyrin may have to oligomerize to create a high-affinity microtubule binding site suitable for anchoring neurotransmitter receptors to specialized tubulin microdomains. Consistent with this idea, binding of gephyrin to polymerized tubulin displays strong cooperativity (7). This cooperative binding may help to nucleate a gephyrin scaffold at developing postsynaptic membrane specializations.

The evolutionary benefit of merging such diverse functions as Moco biosynthesis and receptor clustering is unknown but may be indicative of oxidative functions being required at the synapse. In addition, gephyrin provides another intriguing example of how proteins acquire multifunctionality by recruiting new exonic sequences to appropriate genomic loci. On the other hand, it is tempting to speculate that both Moco biosynthesis and receptor clustering require stringent compartmentalization and that gephyrin may have emerged as organizing molecule for different cellular processes.

We thank I. Bartnik for expert technical assistance, Drs. A. Püschel and J. Kuhse for helpful discussions and critically reading the manuscript, and M. Baier and H. Reitz for secretarial help. This work was supported by Deutsche Forschungsgemeinschaft und Fonds der Chemischen Industrie. J.K. held an endowed professorship of the Stifterverband für die Deutsche Wissenschaft.

1. Pfeiffer, F., Graham, D. & Betz, H. (1982) *J. Biol. Chem.* **257,** 9389–9393.
2. Schmitt, B., Knaus, P., Becker, C.-M. & Betz, H. (1987) *Biochemistry* **26,** 805–811.
3. Prior, P., Schmitt, B., Grenningloh, G., Pribilla, I., Multhaup, G., Beyreuther, K., Maulet, Y., Werner, P., Langosch, D., Kirsch, J. & Betz, H. (1992) *Neuron* **8,** 1161–1170.
4. Triller, A., Cluzeaud, F., Pfeiffer, F., Betz, H. & Korn, H. (1985) *J. Cell Biol.* **101,** 683–688.
5. Sassoè-Pognetto, M., Kirsch, J., Grünert, U., Greferath, U., Fritschy, J. M., Möhler, H., Betz, H. & Wässle, H. (1995) *J. Comp. Neurol.* **357,** 1–14.
6. Todd, A. J., Spike, R. C., Chong, D. & Neilson, M. (1995) *Eur. J. Neurosci.* **7,** 1–11.
7. Kirsch, J., Langosch, D., Prior, P., Littauer, U. Z., Schmitt, B. & Betz, H. (1991) *J. Biol. Chem.* **266,** 22242–22245.
8. Meyer, G., Kirsch, J., Betz, H. & Langosch, D. (1995) *Neuron* **15,** 563–572.
9. Kneussel, M., Hermann, A., Kirsch, J. & Betz, H. (1999) *J. Neurochem.* **72,** 1323–1326.
10. Kirsch, J., Kuhse, J. & Betz, H. (1995) *Mol. Cell. Neurosci.* **6,** 450–461.
11. Kirsch, J. & Betz, H. (1995) *J. Neurosci.* **15,** 4148–4156.
12. Kirsch, J., Wolters, I., Triller, A. & Betz, H. (1993) *Nature (London)* **366,** 745–748.
13. Béchade, C., Colin, I., Kirsch, J., Betz, H. & Triller, A. (1996) *Eur. J. Neurosci.* **8,** 429–435.
14. Kirsch, J. & Betz, H. (1998) *Nature (London)* **392,** 717–720.
15. Essrich, C., Lorez, M., Benson, J. A., Fritschy, J. M. & Lüscher, B. (1998) *Nat. Neurosci.* **7,** 563–571.
16. Feng, G., Tintrup, H., Kirsch, J., Nichol, M. C., Kuhse, J., Betz, H. & Sanes, J. R. (1998) *Science* **282,** 1321–1324.
17. Kneussel, M., Brandstätter, J. H., Laube, B., Stahl, S., Müller, U. & Betz, H. (1999) *J. Neurosci.* **19,** 9289–9297.
18. Betz, H. (1998) *Nat. Neurosci.* **7,** 541–543.
19. Nohno, T., Kasai, Y. & Saito, T. (1988) *J. Bacteriol.* **170,** 4097–4102.
20. Kamdar, K. P., Shelton, M. E. & Finnerty, V. (1994) *Genetics* **137,** 791–801.
21. Stallmeyer, B., Nerlich, A., Schiemann, J., Brinkmann, H. & Mendel, R. R. (1995) *Plant J.* **8,** 751–762.
22. Rajagopalan, K. V. & Johnson, J. L. (1992) *J. Biol. Chem.* **267,** 10199–10202.
23. Stallmeyer, B., Schwarz, G., Schulze, J., Nerlich, A., Reiss, J., Kirsch, J. & Mendel, R. R. (1999) *Proc. Natl. Acad. Sci. USA* **96,** 1333–1338.
24. Ramming, M., Betz, H. & Kirsch, J. (1997) *FEBS Lett.* **405,** 137–140.
25. Johnson, J. L. & Wadman, S. K. (1989) in *Inherited Basis of Metabolic Disease*, ed. Stanbury, J. B. (McGraw–Hill, New York), pp. 1463–1475.
26. Kirsch, J., Malosio, M.-L., Wolters, I. & Betz, H. (1993) *Eur. J. Neurosci.* **5,** 1109–1117.
27. Matzenbach, B., Maulet, Y., Sefton, L., Courtier, B., Avner, P., Guénet, J.-L. & Betz, H. (1994) *J. Biol. Chem.* **269,** 2607–2612.
28. Heck, S., Enz, R., Richter-Landsberg, C. & Blohm, D. (1997) *Dev. Brain Res.* **98,** 211–220.
29. Padgett, R. A, Grabowski, P. J., Konarska, M. M., Seiler, S. & Sharp, P. A. (1986) *Annu. Rev. Biochem.* **55,** 1119–1150.
30. Rivers, S. L., McNairn, E., Blasco, F., Giordano, G. & Boxer, D. H. (1993) *Mol. Microbiol.* **8,** 1071–1081.
31. Krauss, S. & Franke, W. W. (1990) *Gene* **86,** 241–249.
32. Lewis, S., Wang, D. & Cowan, N. J. (1988) *Science* **242,** 936–939.
33. Lee, G., Cowan, N. J. & Kirschner, M. (1988) *Science* **239,** 285–288.
34. Mammoto, A., Sasaki, T., Asakura, T., Hotta, I., Imamura, H., Takahashi, K., Matsuura, Y., Shirao, T. & Takai, Y. (1998) *Biochem. Biophys. Res. Commun.* **243,** 86–89.
35. Sabatini, D. M., Barrow, R. K., Blackshaw, S., Burnett, P. E., Lai, M. M., Field, M. E., Bahr, B. A., Kirsch, J., Betz, H. & Snyder, S. H. (1999) *Science* **284,** 1161–1164.
36. Kins, S., Betz, H. & Kirsch, J. (2000) *Nat. Neurosci.* **3,** 22–29.
37. Dingus, J., Obar, R. A., Hyams, J. S, Goedert, M. & Vallee, R. B. (1991) *J. Biol. Chem.* **266,** 18854–18860.
38. Liu, M., Wuebbens, M., Rajagopalan, K. & Schindelin, H. (2000) *J. Biol. Chem.* **275,** 1814–1822.